

Regiochemically Well-Defined Fluorenone–Alkylthiophene Copolymers: Synthesis, Spectroscopic Characterization, and Their Postfunctionalization with Oligoaniline

Renaud Demadrille,[†] Patrice Rannou,[†] Joël Bleuse,[‡] Jean-Louis Oddou,[§] and Adam Pron^{*,†}

DRFMC, UMR 5819-SPRAM (CEA-CNRS-Univ. J. Fourier-Grenoble I), Laboratoire de Physique des Métaux Synthétiques, DRFMC, SP2M, Laboratoire "Nanophysique et Semiconducteurs", and DRDC, FRE2427 (CEA-CNRS-Univ. J. Fourier-Grenoble I), Laboratoire de Physico-chimie des Métaux en Biologie, CEA Grenoble, 17 Rue des Martyrs 38054 Grenoble Cedex 9, France

Malgorzata Zagorska

Faculty of Chemistry, Warsaw University of Technology, 00 664 Warszawa Noakowskiego 3, Poland

Received March 14, 2003; Revised Manuscript Received June 26, 2003

ABSTRACT: A new solution processable, regioregular, alternate copolymer of fluorenone and dialkylbithiophene, namely poly[(5,5'-(3,3'-di-*n*-octyl-2,2'-bithiophene))-*alt*-(2,7-fluoren-9-one)] (abbreviated as PDOBTF), was synthesized by three different preparation methods: chemical or electrochemical oxidation of 2,7-bis(4-octylthien-2-yl)-fluoren-9-one or polycondensation of 2,7-bis(5-bromo-4-octylthien-2-yl)-fluoren-9-one in the presence of Ni(0) reagent. Independent of the preparation method, the crude product is a mixture of high molecular weight fractions and short oligomers. It can be however easily fractionated into fractions differing in their molecular weight by sequential extractions with a series of solvents. The principal absorption band registered for the undoped polymer ($\lambda_{\max} = 384$ nm for the THF solution and 389 nm for the solid state) originates from the π - π^* transition of the conjugated backbone and is blue-shifted because of the chain torsion effects caused by steric hindrance. This band is accompanied by a peak of smaller intensity ($\lambda_{\max} = 476$ nm for the THF solution and 485 nm for the solid state) attributed to the n - π^* transition in the carbonyl group of the fluoren-9-one subunit. Preliminary photoluminescence studies show that PDOBTF exhibits a very large Stokes shift and emits red light ($\lambda_{\max} = 631$ nm in THF solution and 643 nm in the solid state). Upon chemical p-type doping with FeCl_4^- , the polymer reaches the conductivity of $\sigma_{\text{dc}} = 0.05$ S cm^{-1} . Mössbauer spectroscopy studies of the doping process show that both structural subunits, i.e., the bithiophene subunit and the fluoren-9-one one, participate in the doping. PDOBTF can be relatively easily postfunctionalized by grafting aniline oligomers as pendant groups via the carbonyl groups of the fluoren-9-one subunit. By consequence, the spectrum of the modified polymer can be precisely tuned in the visible region by changing the grafting level.

Introduction

The development of "plastic" electronic devices such as field-effect transistors (FETs),¹ light-emitting diodes (LEDs),² or photovoltaic cells³ resulted in a renewed interest in polyconjugated macromolecular systems observed in the past decade. One of the most important advantages of conjugated polymers is a rather facile tuning of their optical, spectroscopic, and electronic properties by appropriate design of their chain structure and by imposing favorable aggregation of these chains in the solid state via supramolecular engineering. In this paper we report on the first example of a new family of copolymers with conjugated backbone, namely poly[(5,5'-(3,3'-dialkyl-2,2'-bithiophene))-*alt*-(2,7-fluoren-9-one)]s. Poly(fluoren-9-one-2,7-diyl) homopolymer has already been reported in the literature;⁴ however, we were tempted to prepare copolymers of fluoren-9-one with alkyl-substituted thiophenes with the goal to tune its electronic and optical properties and to improve its solution processability. Although being similar to already reported alternating copolymers of fluorene and

dialkylbithiophenes,^{5,6} poly[(5,5'-(3,3'-dialkyl-2,2'-bithiophene))-*alt*-(2,7-fluoren-9-one)]s offer some advantages unobtainable for the former (vide infra).

Our interests in this new family of polyconjugated systems arise from the following reasons:

(i) Their highly regular chain microstructure, which is a simple consequence of the fact that the fluoren-9-one moiety possesses a symmetry axis and the alkyl substituents in the bithiophene unit are regularly distributed via "head-to-head" coupling. Such chain regularity facilitates ordered supramolecular aggregation in the solid state.

(ii) Their luminescent properties combined with solution processability, the latter being assured by the alkyl side groups.

(iii) The possibility of the tuning of their electrical transport properties via chemical or electrochemical doping.

(iv) The possibility of their postpolymerization functionalization via carbonyl groups⁷ present in the polymer main chain. Thus, poly[(5,5'-(3,3'-dialkyl-2,2'-bithiophene))-*alt*-(2,7-fluoren-9-one)]s can be considered, for example, as polymer precursors for the preparation of a whole new series of macromolecules whose absorption spectrum can be precisely tuned via branching appropriate chromophores as side groups. This approach

[†] Laboratoire de Physique des Métaux Synthétiques.

[‡] Laboratoire "Nanophysique et Semiconducteurs".

[§] Laboratoire de Physico-chimie des Métaux en Biologie.

* To whom the correspondence should be addressed: Tel 33-4-38784389; Fax 33-4-38785113; e-mail pron@cea.fr.

is of extreme importance in view of the use of conjugated polymers as components of organic solar cells^{8–10} since it may result in a much better match between the solar radiation and the polymer absorption, leading in turn to much better device efficiency.

In the first part of the paper we describe the synthesis of poly[(5,5'-(3,3'-di-*n*-octyl-2,2'-bithiophene))-*alt*-(2,7-fluoren-9-one)] (PDOBTF) and characterize its principal properties in the undoped state. In the second part we focus on its p-type doping using FeCl₃ as the doping agent and on the characterization of the doped polymer by elemental analysis, dc conductivity measurements, and Mössbauer spectroscopy. Finally, we give an example of postpolymerization functionalization of the above copolymer with the goal to demonstrate that its UV–vis spectrum can be tuned by grafting aniline tetramer to the conjugated main chain via the carbonyl group present in the fluoren-9-one moiety.

Experimental Section

Reagents and Chemicals. All reagents and chemicals were purchased from Aldrich. Chloroform and nitromethane were dried over CaCl₂ and distilled in a vacuum line prior to the use. FeCl₃ was dried in a high-vacuum line by dynamic pumping at the temperature of 60 °C for 2 h. Other reagents and chemicals were used as received.

Characterization Techniques. All synthesized monomers and polymers in the undoped state were characterized by ¹H and ¹³C NMR and elemental analysis. Undoped polymers were also characterized by Fourier transform infrared (FT-IR) and ultraviolet–visible (UV–vis) absorption spectroscopies. Polymers doped with FeCl₃ were subjected to elemental analysis, room temperature dc conductivity measurements, and ⁵⁷Fe Mössbauer spectroscopy.

NMR were recorded on a Bruker AC 200 MHz or on a Varian 400 MHz spectrometer. Acetone-*d*₆ or chloroform-*d* (CDCl₃) containing TMS as an internal standard were used as solvent depending on the solubility of the material.

Elemental analyses (C, H, N, and S in the case of monomers and undoped polymers and additionally Fe and Cl in the case of FeCl₄[−]-doped samples) were carried out by the Analytical Service of CNRS Vernaison (France).

FT-IR spectra of undoped polymers were recorded on a Perkin-Elmer paragon500 spectrometer (wavenumber range: 400–4000 cm^{−1}; resolution: 2 cm^{−1}) using the KBr pellet technique. Solution (THF) and solid-state (thin films cast from THF solutions) UV–vis absorption spectra were recorded in situ during the SEC analyses using the diode array UV–vis spectrometer of the 1100HP Chemstation and on a Perkin-Elmer Lambda 2 spectrometer, respectively.

Molecular weight determinations of polymer fractions studied were measured using size exclusion chromatography (SEC) on a 1100HP Chemstation equipped with a 300 × 7.5 mm PLgel Mixed-D 5 μm/10⁴ Å column. Detection was performed by a diode array UV–vis detector and a refractive index detector. The column temperature and the flow rate were fixed to 313 K and 1 mL min^{−1}, respectively. The calibration curve was built using 10 polystyrene (PS) narrow standards (S-M-10* kit from Polymer Labs). Two runs of 20 μL injection of ca. 2 mg mL^{−1} polymer in HPLC grade THF solutions were typically analyzed for each sample with a UV–vis detection located at 355 nm.

Mass spectra were acquired on a LCQ-ion trap ThermoFinnigan spectrometer equipped with an electrospray source (MS-ESI). Electrospray full scan spectra, in the range of *m/z* 180–300 *uma*, were obtained by infusion through fused silica tubing at 2–10 μL min^{−1}. The solutions (CH₂Cl₂) were analyzed in the positive mode. The LCQ calibration (*m/z* 50–2000) was achieved according to the standard calibration from the manufacturer (mixture of caffeine, MRFA, and ultramark 1621). The temperature of the heated capillary of the LCQ was set to 433 K.

Photoluminescence measurements of monomers and undoped polymers were carried out on a Jobin-Yvon HR 460 monochromator equipped with a CCD silicium detector cooled at 140 K. Excitation was performed with an argon laser at 303, 365, and 458 nm.

The dc conductivity (σ_{dc} [S cm^{−1}]) measurements of the doped polymer films were performed at room temperature (RT), on pressed pellets, in a standard four-probe geometry, using pressure contacts.

Mössbauer spectra of FeCl₃-doped polymers were measured at 4.2 K. The samples were loaded in a drybox into a tight polyamide container prior to the experiment and immediately transferred to the cryostat of the spectrometer. A typical thickness of the absorber was 5 mg cm^{−2} of natural iron. Co-(Rh) was used as a Mössbauer source. An α -Fe absorber operating at RT was used for the velocity calibration. The spectra were recorded in a constant acceleration mode and analyzed in a least-squares procedure.

Synthesis. 5,5-Dimethyl-2-(4-octylthien-2-yl)[1,3,2]dioxaborinane (1). 6.8 mL (11 mmol) of *n*-butyllithium in a form of 1.6 M solution in hexane was added dropwise, at −50 °C during 5 min, to a stirred solution of 1.96 g (10 mmol) of 3-*n*-octylthiophene in dry THF (20 mL). The color of the mixture became slightly yellow. The mixture was additionally stirred for 60 min at −50 °C and then cooled to −78 °C. At this stage 9 mL (33 mmol) of tributylborate was added quickly to the reaction vessel, and the solution was allowed to warm to RT. Upon warming the reaction mixture became milky. It was then poured into 1 M HCl containing ice (40 mL) and then extracted with diethyl ether. The organic layer was washed twice with brine and dried over magnesium sulfate in the presence of 5.20 g (50 mmol) of neopentyl glycol for 30 min. Subsequent separation of the drying agent by filtration and removal of the solvent, using a rotary evaporator, gave a transparent oil. Further purification by silica gel column chromatography with a hexane–ether mixture (9:1) as eluent afforded 2.34 g of a light yellow oil (yield 76%). ¹H NMR (acetone-*d*₆, 200 MHz, ppm): δ 7.36 (d, 1H, *J* = 1.21 Hz), 7.28 (d, 1H, *J* = 1.08 Hz), 3.76 (s, 4H), 2.63 (t, 2H, *J* = 7.8 Hz), 1.58–1.65 (m, 2H), 1.32–1.25 (m, 10H), 1.01 (s, 6H), 0.89–0.84 (m, 3H). ¹³C NMR (acetone-*d*₆, 200 MHz, ppm): 146.01, 138.71, 128.37, 73.72 (2C), 33.60, 32.52, 31.56, 31.12, 31.00, 30.81, 30.42, 24.30, 22.87 (2C), 15.32, *C*-Boron not observed. Elemental analysis: Calcd for C₁₇H₂₉BO₂S: C, 66.23%; H, 9.48%; S, 10.40%. Found: C, 64.90%; H, 9.46%; S, 9.26%.

2,7-Bis(4-octylthien-2-yl)fluoren-9-one (2). 436 mg of 2,7-dibromofluoren-9-one (1.29 mmol) and 890 mg of compound **1** (2.88 mmol) were placed in anhydrous DMF (8 mL). The mixture was stirred under argon for 10 min, and then 610 mg of K₃PO₄ (2.87 mmol) and 150 mg of Pd[P(Ph)₃]₄ (0.129 mmol) in 8 mL of DMF were added. The mixture was kept for an additional period of 12 h at 85 °C with constant stirring and then allowed to cool to RT. At this stage 10 mL of diethyl ether was added. After filtration an orange, strongly fluorescent solid was recovered. This solid was then washed twice with ether and then with pentane. The product was then separated from K₃PO₄ by dissolving in dichloromethane. The solvent was removed using a rotary evaporator to give 480 mg of the product (yield 65.4%). ¹H NMR (CDCl₃, 200 MHz, ppm): δ 7.88 (d, 2H, *J* = 1.61 Hz), 7.68 (dd, 2H, *J* = 7.79 and 1.74 Hz), 7.47 (d, 2H, *J* = 7.79 Hz), 7.22 (d, 2H, *J* = 1.34 Hz), 6.90 (d, 2H, *J* = 1.07 Hz), 2.61 (t, 4H, *J* = 7.39 Hz), 1.56–1.70 (m, 4H), 1.20–1.40 (m, 20H), 0.85–0.92 (m, 6H). ¹³C NMR (CDCl₃, 200 MHz, ppm): 193.39 (C=O), 144.57 (2C), 142.67 (2C), 142.61 (2C), 135.64 (2C), 135.09 (2C), 131.46 (2C), 125.13 (2C), 121.37 (2C), 120.66 (2C), 120.18 (2C), 31.86 (2C), 30.59 (2C), 30.42 (2C), 29.40 (2C), 29.32 (2C), 29.22 (2C), 22.65 (2C), 14.05 (2C). Elemental analysis: Calcd for C₃₇H₄₄OS₂: C, 78.12%; H, 7.80%; S, 11.27%. Found: C, 77.86%; H, 7.83%; S, 11.46%.

2,7-Bis(5-bromo-4-octylthien-2-yl)fluoren-9-one (3). A solution of **2** (545 mg (0.96 mmol) in 10 mL of chloroform) was slowly added to a solution of *N*-bromosuccinimide (NBS) (427 mg (2.40 mmol) in 10 mL of the same solvent). The mixture was stirred overnight at RT under argon. It was then washed with water, and the organic layer was dried over magnesium

sulfate and filtered. Evaporation of the solvent followed by recrystallization of the product from chloroform/methanol afforded 540 mg of an orange solid (yield 77.5%). ¹H NMR (CDCl₃, 200 MHz, ppm): δ 7.74 (dbr, 2H, *J* = 1.61 Hz), 7.56 (dd, 2H, *J* = 7.80 and 1.75 Hz), 7.41 (dbr, 2H, *J* = 7.80 Hz), 7.04 (s, 2H), 2.54 (t, 4H, *J* = 7.26 Hz), 1.53–1.64 (m, 4H), 1.26–1.32 (m, 20H), 0.85–0.92 (m, 6H). ¹³C NMR (CDCl₃, 200 MHz, ppm): 192.93 (C=O), 143.44 (2C), 142.78 (2C), 142.14 (2C), 134.82 (2C), 135.06 (2C), 134.82 (2C), 131.15 (2C), 124.60 (2C), 120.90 (2C), 120.83 (2C), 109.11 (2C), 31.86 (2C), 29.65 (4C), 29.36 (2C), 29.24 (2C), 29.21 (2C), 22.65 (2C), 14.06 (2C). Elemental analysis: Calcd for C₃₇H₄₂Br₂OS₂: C, 61.16%; H, 5.83%; S, 8.83%. Found: C, 61.53%; H, 5.83%; S, 8.51%.

Poly[(5,5'-(3,3'-di-*n*-octyl-2,2'-bithiophene))-*alt*-(2,7-fluorene-9-one)] (PDOBTF). *Method A.* A solution of 530 mg of anhydrous ferric chloride (4.18 mmol) in a mixed solvent consisting of 5 mL of nitromethane and 30 mL of chloroform was added dropwise to a solution of **2** (450 mg, 0.79 mmol) in 30 mL of freshly distilled and degassed chloroform. The addition was performed at 0 °C with constant stirring over a period of 90 min. At the end of the addition, the mixture was warmed to 10 °C and was maintained at this temperature for an additional period of 60 min. The reaction mixture was then allowed to warm to RT and stirred for 12 h. Subsequently, it was concentrated by pumping under vacuum and then precipitated in 100 mL of methanol. The crude polymer was then dissolved in 50 mL of chloroform and washed four times with a 0.1 M aqueous solution of ammonia (150 mL each time). In the next step the polymer was stirred for 48 h with the same aqueous solution. As-synthesized polymer usually contains minute amounts of dopants of unidentified chemical nature and requires further dedoping. The dedoping was achieved by washing the chloroform solution of the polymer with an EDTA aqueous solution (0.05 M, 200 mL). The polymer was then washed with water twice and then dried under vacuum to give 327 mg of a red-brown powder (yield 73%). ¹H NMR (CDCl₃, 200 MHz, ppm): δ: 7.78 (sbr, 2H), 7.59 (d, *J* = 7.6 Hz, 2H), 7.35 (d, *J* = 7.8 Hz, 2H), 7.19 (s, 2H), 2.53 (m, 4H), 1.55 (m, 4H), 1.18 (m, 20H), 0.80 (m, 6H). ¹³C NMR (CDCl₃, 200 MHz, ppm): δ: 193.29 (C=O), 144.55 (2C), 143.8 (2C), 142.59 (2C), 135.11 (2C), 131.34 (2C), 128.71 (2C), 125.48 (2C), 125.13 (2C), 121.11 (2C), 120.70 (2C), 31.89 (2C), 30.32 (2C), 29.67 (4C), 29.42 (2C), 29.24 (2C), 22.66 (2C), 14.08 (2C). IR (KBr, cm⁻¹): 3054 (w), 2953 (m), 2924 (s), 2852 (s), 1720 (s), 1601 (w), 1583 (w), 1537 (w), 1472 (s), 1434 (m), 1376 (w), 1292 (w), 1260 (w), 1161 (w), 1124 (w), 1026 (w), 823 (m), 785 (m). Elemental analysis: Calcd for C₃₇H₄₄OS₂: C, 78.12%; H, 7.80%; S, 11.27%. Found: C, 77.10%; H, 7.70%; S, 9.95%.

Method B. In a one-compartment, three-electrode electrochemical cell equipped with a flat platinum working electrode (3 mm²), a Pt wire counter electrode, and an Ag/AgNO₃ reference electrode, 10 mL of the electrolyte composed of 0.1 M tetrabutylammonium tetrafluoroborate solution in dichloromethane was placed, and the cell was purged with argon for 10 min. 11.36 mg (0.02 mmol) of monomer **2** was added to this electrolyte solution to obtain 2 × 10⁻³ M concentration with respect to **2**. The film was produced by consecutive potential cycling (100 scans) in the range from -0.2 to +0.9 V vs Ag/Ag⁺ with the scan rate of 100 mV s⁻¹. The deposited polymer was then reductively dedoped by cycling 50 times in the potential range of 0.0 to -0.2 V with the same scan rate. The reduced (undoped) polymer deposited on the Pt working electrode was then washed with acetonitrile, dried, and finally dissolved in THF. This solution was then used for the SEC characterization of the electrochemically synthesized polymer.

Method C. Ni(COD)₂ (218 mg, 0.79 mmol), COD (72 mg, 0.66 mmol), and 2,2'-bipyridyl (124 mg, 0.79 mmol) were mixed together in 10 mL of anhydrous DMF. The solution was then heated at 55 °C for 40 min and then slowly added (over 20 min) to a solution of **3** (480 mg, 0.66 mmol) in dry THF (10 mL) kept at the same temperature. The mixture was then maintained at 55 °C under stirring in the dark for 48 h. It was then allowed to cool to RT and precipitated with 300 mL of methanol. The precipitate was filtered and dried under dynamic vacuum to provide 355 mg of a red powder (yield:

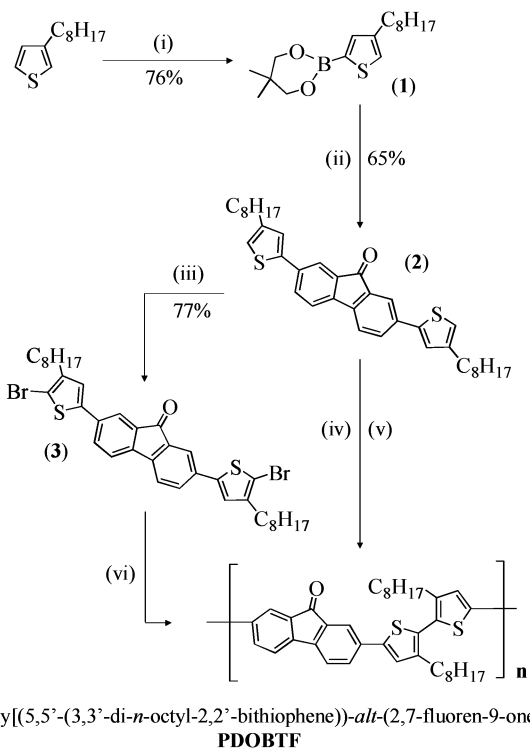
95%). ¹H NMR (CDCl₃, 400 MHz, ppm): δ: 7.91 (m, 2H), 7.69 (m, 2H), 7.49 (m, 2H), 7.29 (s, 2H), 2.60 (t, 4H, *J* = 8 Hz), 1.64 (m, 4H), 1.27 (m, 20H), 0.87 (m, 6H). ¹³C NMR (CDCl₃, 200 MHz, ppm): δ: 193.18 (C=O), 143.75 (2C), 142.60 (2C), 142.35 (2C), 135.07 (2C), 131.34 (2C), 128.76 (2C), 125.42 (2C), 125.12 (2C), 121.05 (2C), 120.66 (2C), 31.92 (2C), 30.72 (4C), 29.45 (4C), 29.24 (2C), 22.66 (2C), 14.08 (2C). IR (KBr, cm⁻¹): 3054 (w), 2953 (m), 2924 (s), 2852 (s), 1720 (s), 1601 (w), 1583 (w), 1537 (w), 1472 (s), 1434 (m), 1376 (w), 1292 (w), 1260 (w), 1161 (w), 1124 (w), 1026 (w), 823 (m), 785 (m). Elemental analysis: Calcd for C₃₇H₄₄OS₂: C, 78.12%; H, 7.80%; S, 11.27%. Found: C, 76.41%; H, 7.38%; S, 10.74%.

UV-vis Spectroelectrochemistry of Chemically Polymerized PDOBTF. For spectroelectrochemical investigations a thin layer of the polymer (method A) was deposited on an ITO transparent electrode by casting from a THF solution. The experiments were carried out in a one-compartment spectroelectrochemical cell using a Pt counter electrode and an Ag/0.1 M AgNO₃ reference electrode. A 0.1 M solution of tetrabutylammonium tetrafluoroborate solution in acetonitrile was used as the electrolyte.

Chemical Doping of PDOBTF. Chemical doping with FeCl₃ was carried out for the polymer prepared by method A using a standard high-vacuum line technique. In a typical procedure an appropriate amount of dry nitromethane was distilled in a vacuum line to the sidearm of the doping reactor containing vacuum-dried FeCl₃ as to give a 0.3 M doping solution. This solution was then transferred to the main arm of the reactor and kept in contact with the polymer film for 2 h. During the doping reaction the film, floating initially on the surface of the doping solution, fell to the bottom of the reactor which was caused by the doping-induced increase of the polymer density. The excess of the unreacted FeCl₃, as well as side-reaction products, was removed by repeated washing with small amounts of dry nitromethane. Finally, the polymer was pumped in a high-vacuum line for 2 h.

Grafting of Aniline Tetramer to PDOBTF Main Chain: PDOBTF-4EB1 and PDOBTF-4EB2. Aniline tetramer in the oxidation state of emeraldine (4EB), which is not commercially available, was prepared using a modification of the method described in ref 11. The exact preparation procedure used in this research can be found elsewhere.¹²

Grafting of the tetramer to the PDOBTF main chain can briefly be described as follows. 86 mg of PDOBTF (0.15 mmol) obtained by oxidative polymerization (dichloromethane fraction *M_n* = 5.48 kDa equiv PS and *M_w*/*M_n* = 2.01) were dissolved in 15 mL of hot dry toluene under argon. 100 mg (0.27 mmol) of aniline tetramer was added, and the resulting mixture was cooled to 0 °C. 34 mg (0.18 mmol) of TiCl₄ was then added dropwise, and the solution turned instantaneously greenish. The mixture was left under stirring at 0 °C for an additional 10 min and then allowed to warm to RT. In the next step it was heated at 110 °C overnight. After this period the reaction mixture was cooled to RT and concentrated using a rotary evaporator. After precipitation from methanol (350 mL), the crude polymer (black powder) was recovered by filtration. It should be noted here that, due to the acidity of the reaction mixture, the oligoaniline side groups grafted to the PDOBTF main chain are "doped" or, in other words, protonated and by consequence must be dedoped, i.e., transformed from their salt form to the base form. The dedoping was performed by stirring the crude polymer in 50 mL of 0.05 M aqueous solution of ammonia for 15 h. The dedoped polymer was then separated by filtration and washed consecutively with water, 200 mL of methanol, and 200 mL of acetone to remove the remaining traces of "free" aniline tetramer which were not grafted to PDOBTF. The polymer with grafted oligoaniline side groups was separated into two fractions: the "low grafting" level fraction which was extracted with CHCl₃ in a Soxhlet apparatus (PDOBTF-4EB1) and the high grafting level fraction which remained insoluble (PDOBTF-4EB2). This fraction was then dried under vacuum to yield 90 mg of a black powder (65% yield). IR (KBr, cm⁻¹): 3340 (w), 3013 (w), 2940 (m), 2916 (s), 2847 (s), 1717 (w), 1588 (s), 1494 (s), 1461 (s), 1376 (m),

Scheme 1. Chemical Formulae of 1, 2, 3, and PDOBTF and Their Synthesis Pathways^a


^a Reagents and conditions: (i) BuLi, THF; B(OC₄H₉)₃, -78 °C; neopentyl glycol, ether; (ii) 0.5 equiv of 2,7-dibromofluoren-9-one, Pd[P(Ph)₃]₄, K₃PO₄, DMF, 85 °C; (iii) 2 NBS, CHCl₃; (iv) chemical oxidative polymerization (method A): FeCl₃, CHCl₃/CH₃NO₂, 0 °C; (v) electrochemical polymerization (method B): CH₂Cl₂, Bu₄NBF₄; (vi) polycondensation polymerization (method C): Ni(COD)₂, COD, Bpy, THF/DMF, 55 °C, 48 h.

1291 (m), 1252 (m), 1157 (m), 1124 (m), 1026 (w), 906 (w), 818 (m), 783 (w), 744(w), 693 (w).

Results and Discussion

Synthesis. Suzuki or Stille coupling are among the most popular synthetic routes for the preparation of conjugated copolymers. They can be used directly in the copolymerization reaction^{5,13,14} or alternatively in the preparation of monomers combining building blocks originating from different homopolymers. Such "hybrid-type" monomers can then be polymerized by other methods to give copolymers with well-defined regiochemistry.^{5,6} In the presented research we have exploited the latter approach. The exact synthetic strategy is based on the synthesis of a symmetric monomer containing fluoren-9-one and 3-*n*-octylthiophene units which upon homocoupling give polymer chains with regioregular head-to-head sequence of the alkyl substituents. Both the synthesis of the monomer and its polymerizations are outlined in Scheme 1. Monomer **2**, 2,7-bis(4-octylthien-2-yl)-fluoren-9-one, can be obtained from 2,7-dibromofluoren-9-one which is commercially available and 5,5-dimethyl-2-(4-octylthien-2-yl)[1,3,2]-dioxaborinane (**1**) prepared according to the literature method.¹⁵ The reaction involves Suzuki coupling with palladium tetrakis(triphenylphosphine) (Pd[P(Ph)₃]₄) as the catalyst. Direct bromination of **2** with *N*-bromosuccinimide affords **3** in good yield.¹⁶ Both **2** and **3** can be polymerized to give PDOBTF (see Scheme 1). Oxidative polymerization of **2** can be carried out chemically using FeCl₃ as the oxidizing agent or electrochemically. When

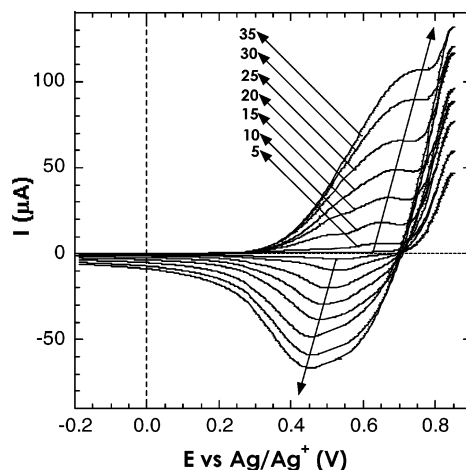


Figure 1. Selected cyclic voltammograms (scan numbers are indicated in the figure) corresponding to voltammetric electropolymerization of **2** (2×10^{-3} M). Scan rate 100 mV s^{-1} (E vs Ag/0.1 M AgNO₃, electrolyte 0.1 M Bu₄NBF₄ in dichloromethane). The two arrows showing the oxidation (arrow pointing upward) and reduction (arrow pointing downward) waves are only guidelines.

applying the former, it is convenient to use Andersson's procedure¹⁷ yielding, in many cases, higher molecular weight polymers. In this method the potential of the oxidative couple is adjusted by the Fe³⁺/Fe²⁺ ratio following the Nernst equation. As a result, the polymerization can be carried out at relatively mild conditions without overoxidation effects. Electrochemical oxidative polymerization can be carried out either with constant current or with constant potential or by potential scanning (voltammetric electropolymerization). Since the potential control is of crucial importance in view of the possibility of overoxidation effects, the latter two methods are preferable. Cyclic voltammetry scans accompanying the voltammetric electropolymerization of **2** are shown in Figure 1. In addition to the onset of the irreversible polymerization peak, a redox couple increasing in intensity with each consecutive scan can clearly be seen. This couple is associated with the doping and dedoping of the polymer deposited on the electrode. PDOBTF can also be prepared via polycondensation of **3**. This method is, in reality, based on Yamamoto's coupling^{18,19} using zerovalent nickel reagent, bis(1,5-cyclooctadiene)nickel(0), Ni(COD)₂, in the presence of 1,5-cyclooctadiene (COD) and 2,2'-bipyridyl (Bpy). Recently,²⁰ it has been found that the difference in the sequence of the reagents and catalyst addition is of crucial importance for obtaining high molecular weight polymers. Inspired by the data presented in ref 17, we have carried out the polycondensation reaction by slowly adding the hot nickel catalyst dissolved in DMF to the monomer solution in THF. This order of additions essentially eliminates the formation of the dinickel-substituted complex which is known to be unstable and to undergo hydrolysis or decomposition,²¹ ending, in this manner, the chain propagation. Since chain termination can also be caused by the polymer precipitation, we have changed the solvent, in comparison to the original procedure described in ref 20, with the goal to increase the solubility of the polymer in the reaction medium.

Molecular Weight. In a comparative study of the preparation of new polymers by three different methods, the first problem to be addressed is the influence of the preparation procedure on the molecular weight of the resulting polymer and its distribution. SEC chromatography

Table 1. MS-ESI vs SEC Characterizations of Monomer **2** and of the Ether Fraction of PDOBTF (Method A: Chemical Oxidative Polymerization)^a

oligomers	absolute mass	<i>m/z</i> from MS-ESI	<i>M</i> _{peak} (Da equiv PS) from SEC	<i>F</i> _{corr}
monomer 2	568.28	568.3	299.6	0.53
dimer	1134.55	1134.6	913.4	0.81
trimer	1700.82	1700.9	1645.1	0.97
tetramer	2267.09	1134.7 (2+)	2546.7	1.12
pentamer	2833.35	1417.7 (2+)	3645.6	1.55

^a *m/z* denotes the mass obtained from MS-ESI, *M*_{peak} denotes the molecular weight at the peak apex obtained from SEC, and *F*_{corr} is the correction factor.

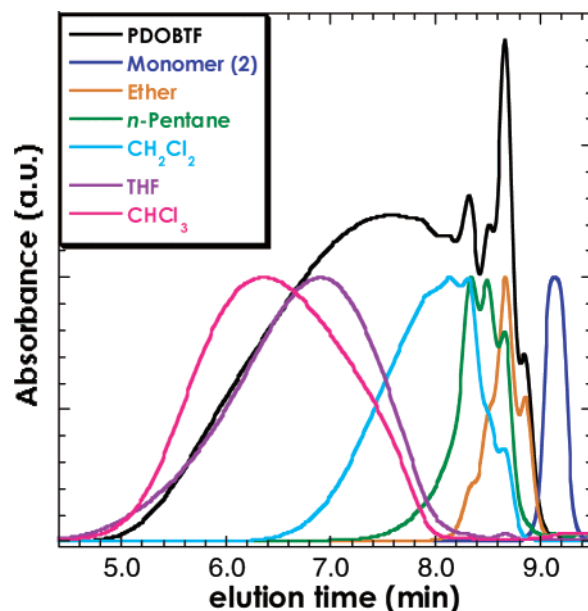
grams of crude polymers, independent of the polymerization method used, are rather complex and on their longer retention time side consist of several sharp peaks. Mass spectrometry (MS-ESI) investigations carried out, for the ether and acetone fractions, in parallel to the SEC ones, unequivocally show that the above-mentioned peaks correspond to oligomers that from dimer to pentamer give clear maxima in the chromatograms. In contrast to SEC, mass spectrometry gives access to absolute values of the molecular weight. Thus, a comparison of the mass spectrometry data with those obtained using SEC with polystyrene standards provides the values of the correction factors (*F*_{corr}) for the chromatographic determination of the molecular weight of the polymer under investigation. The results of this comparative study are summarized in Table 1. The correction factor determined as the ratio of *M*_{n(SEC)}/*M*_{n(MS-ESI)} increases with the increase of *M*_{n(MS-ESI)} from 0.81 to 1.55 in the range of the molecular weights studied. This means that for short oligomers the SEC method underestimates the molecular weight whereas for longer ones it overestimates it with the cross-over from underestimation to overestimation around *M*_{n(MS-ESI)} = 2000 g mol⁻¹. Interestingly, for comparable molecular weights, the calculated correction factors determined here for PDOBTF are very similar to those determined for regioregular poly(3-hexylthiophene-2,5-diyl) (P3HT) by comparison of MALDI-TOF and SEC data.²²

As already stated, crude polymers can be considered as a mixture of oligomeric and polymeric species. *M*_n, *M*_w, and polydispersity coefficients determined for crude polymers using polystyrene standards are collected in Table 2. One should note that the crude polymers, independent of whether they are obtained by chemical oxidative polymerization of **2** or by polycondensation of **3**, show rather large polydispersity coefficients. For this reason we have undertaken the task of their fractionation not only with the goal to remove the oligomer fractions but also to obtain polymer fractions with significantly lower polydispersity. Few papers have been published on the fractionation of poly(thiophene) derivatives.^{23–25} In particular, in ref 23 an efficient method for the fractionation of regioregular P3HT has been proposed, leading to relatively sharp polymer fractions. The method is based on sequential extractions of the fractions with increasing molecular weight using an experimentally determined series of solvents. For the purpose of this research we have slightly modified the original procedure used for regioregular P3HT. In particular, the crude polymer was first extracted with ether in a Soxhlet apparatus until the filtrate was colorless. The remaining part, insoluble in ether, was then consecutively extracted with acetone, *n*-pentane,

Table 2. Macromolecular Parameters of Crude Polymers (Method A: Chemical Oxidative Polymerization; Method B: Electrochemical Polymerization (Bold); Method C: Polycondensation Polymerization (Italic)), and Their Fractions Obtained by Sequential Extractions^a

	<i>M</i> _n (kDa equiv PS)	<i>M</i> _w (kDa equiv PS)	<i>M</i> _w / <i>M</i> _n	abundance (wt %)
crude				
PDOBTF-A	4.99	31.55	6.32	100
PDOBTF-B	5.88	12.82	2.18	100
<i>PDOBTF-C</i>	<i>2.26</i>	<i>7.29</i>	<i>3.23</i>	<i>100</i>
ether-A	1.30	1.72	1.33	20.70
ether-C	0.79	1.37	1.72	7.75
acetone-A	1.85	2.46	1.33	2.40
acetone-C	2.17	3.99	1.84	1.40
<i>n</i> -pentane-A	2.32	3.64	1.57	0.40
<i>n</i> -pentane-C	1.94	2.21	1.15	0.80
CH ₂ Cl ₂ -A	5.48	11.0	2.01	33.00
CH ₂ Cl ₂ -C	4.82	6.77	1.40	24.75
THF-A	28.50	62.87	2.21	31.50
THF-C	<i>b</i>	<i>b</i>	<i>b</i>	8.75
CH ₂ Cl ₃ -A	41.01	74.11	1.81	12.00
CHCl ₃ -C	13.27	19.20	1.45	56.55

^a *M*_n denotes number-average molecular weight, *M*_w weight-average molecular weight, and *M*_w/*M*_n the polydispersity coefficient. The abundance of each fraction in the crude polymer is expressed in wt %. ^b Degraded after prolonged storage at RT.

**Figure 2.** SEC elugrams of monomer **2**, of the crude polymer PDOBTF prepared by chemical oxidative polymerization (method A), and of its fractions obtained by consecutive Soxhlet extractions (ether, acetone, *n*-pentane, CH₂Cl₂, THF, CHCl₃). The SEC elugram of the acetone fraction is omitted for clarity reasons.

dichloromethane, tetrahydrofuran, and chloroform in the same manner as in the case of the extraction with ether. Macromolecular parameters of all fractions obtained by sequential extractions are collected in Table 2. In the last column the content of each fraction in the crude polymers, expressed in wt %, is indicated. The elution curves recorded for monomer **2**, the crude polymer (method A), and each fraction are shown in Figure 2.

It is clear that the ether, acetone, and *n*-pentane fractions, which account for ca. 23 wt % of the polymer prepared by method A, are in reality mixtures of oligomers. The fractions obtained by extraction with THF and chloroform exhibit the highest molecular

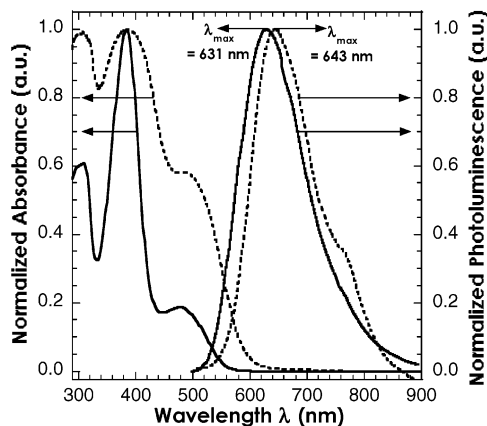


Figure 3. UV-vis and photoluminescence (PL: $\lambda_{\text{exc}} = 365$ nm) solution (—) and solid state (---) spectra of the THF fraction of PDOBTF prepared by method A.

Table 3. UV-vis and Photoluminescence (PL) Data of Monomer 2, PDOBTF, and Its Oligomers (THF Solutions and Thin Solid Film)

	λ_{max} (nm) $\pi-\pi^*$ transition	λ_{max} (nm) $n-\pi^*$ transition	λ_{max} PL (nm) ($\lambda_{\text{exc}} = 365$ nm)
monomer 2	370	468	608
dimer	374	476	
trimer	376	476	
tetramer	378	476	
pentamer	380	476	
CH ₂ Cl ₂	382	476	629
THF	384	476	631
CHCl ₃	384	476	631
film	389	485	643

weight. Again, it should be pointed out that M_n and M_w listed in Table 2, for all fractions higher than the acetone one, are overestimated.

Optical and Spectroelectrochemical Properties.

THF solution and solid-state absorption as well as photoluminescence spectra of PDOBTF prepared by method A are presented in Figure 3. In the absorption spectrum, measured in solution, three clear bands can be distinguished at 310, 384, and 476 nm. We assign the band at 384 nm to the $\pi-\pi^*$ transition in the conjugated backbone of the copolymer. The position of this band is slightly hypsochromically shifted as compared to the corresponding band recorded for poly[(5,5'-(3,3'-dialkyl-2,2'-bithiophene))-*alt*-(2,7-(9,9-dialkylfluorene))], i.e., the polymer analogous PDOBTF but containing two alkyl groups at the 9-position instead of the carbonyl group.⁵ Following the assignment proposed in ref 4 for poly(flouren-9-one-2,7-diyl) homopolymer, we attribute the band at 476 nm to the $n-\pi^*$ transition of the carbonyl group. UV-vis absorption spectroscopy data for the oligomers and for the highest molecular weight fractions of PDOBTF prepared by method A are collected in Table 3 and compared with that recorded, in the same solvent (THF), for the monomer, i.e., 2,7-bis(4-octylthien-2-yl)-fluoren-9-one (**2**). The increase in the chain length results in a continuous bathochromic shift of the $\pi-\pi^*$ band, as expected. Beginning from the THF fraction, no further increase of this shift is observed, consistent with the SEC results which show that for these fractions no contribution from the oligomeric species exists.

A large bathochromic shift (>80 nm) of the peak corresponding to the $n-\pi^*$ transition in the carbonyl group for both the monomer and PDOBTF in comparison to the analogous band in fluoren-9-one molecule⁴

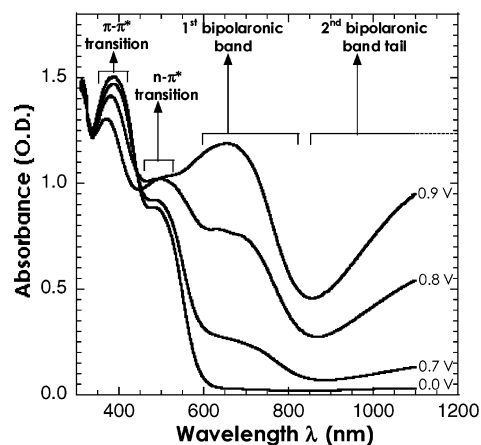


Figure 4. UV-vis-NIR spectroelectrochemical data recorded for thin solid film of PDOBTF (method A, THF fraction) deposited on an ITO electrode (E vs Ag/0.1 M AgNO₃, electrolyte 0.1 M Bu₄NBF₄ in acetonitrile).

should be noted here. This shift can be interpreted as a result of the conjugation of the carbonyl group with a delocalized π -bonding system which in the case of the monomer must extend to the thiophene units. The $n-\pi^*$ band is very little dependent on the chain length. It bathochromically shifts when going from the monomer to the dimer, and then its position stabilizes.

In our further investigations we have used UV-vis-NIR spectroelectrochemistry with the goal to corroborate the above-proposed assignments. The spectra recorded at increasing electrode potentials are presented in Figure 4. First, we note that the absorption bands measured for the thin solid film are significantly broadened as compared to those recorded for the solution spectrum. Moreover, they are bathochromically shifted to ca. 389 and 485 nm, i.e., by 5 and 9 nm with respect to their positions in the solution spectrum. Such a behavior is indicative of a small solvatochromic effect. Solvatochromism is a common phenomenon in alkylthiophene-based conjugated polymers.²⁶ The hypsochromic shift in the position of the bands occurring upon the dissolution of the polymer is caused by macromolecule-solvent interactions which change the conformation of the chain from more planar in the solid state to less planar in solution. In the latter the conjugation is less pronounced since the overlap of p_z orbitals is less effective.

Before the interpretation of the spectroelectrochemical data a short comment is needed. Electrochemical oxidative doping of conjugated polymers with non-degenerated ground state gives rise to a bleaching of the band corresponding to the $\pi-\pi^*$ transition in the conjugated backbone of the polymer. Simultaneously, three (or two) bands grow in the less energetic part of the spectrum associated with the formation of radical cations (polarons) or dication (bipolarons), respectively. In this perspective the doping of PDOBTF should only involve the aromatic π -system of the polyconjugated backbone of the polymer chain, leaving the carbonyl group intact. As seen from Figure 4, first spectroscopic indications of the doping process appear at the potential of $E = 0.7$ V. The doping is manifested by a small decrease of the band at 389 nm and the appearance of a band at ca. 650 nm accompanied by a second band in the near-infrared part of the spectrum, whose onset is seen in Figure 4 in the form of steadily increasing absorbance in the spectral range 850–1100 nm. Further

increase of the electrode potential results in a gradual bleaching of the band at 389 nm. To the contrary, with the increasing electrode potential, the band at 485 nm increases in intensity. The apparent growth of this band is caused by the fact that it is superimposed on the low-energy tail of the first doping-induced band whose intensity grows with increasing doping level. Thus, the spectroelectrochemical behavior of our copolymer is consistent with the band assignment proposed in ref 4 for poly(fluoren-9-one-2,7-diyl) homopolymer with the band at 389 nm attributed to the $\pi-\pi^*$ transition in the polyconjugated chain and the band at 485 nm to the $n-\pi^*$ transition of the carbonyl group.

To better characterize the newly synthesized polymer, we have registered its photoluminescence spectra. Since the presented results are only qualitative, they must be considered as preliminary. Solution photoluminescence spectra of PDOBTF show one clear peak at 631 nm whose shape and position are independent of the energy of excitation line (see Table 3 and Figure 3). In the solid state the emission band is bathochromically shifted by 12 nm. A comparison of the positions of the luminescence peak of the monomer, i.e., 2,7-bis(4-octylthien-2-yl)-fluoren-9-one (**2**), and the polymer shows that the polymerization induces a significant bathochromic shift of 25 nm, much higher than that observed in the absorption spectra (vide supra).

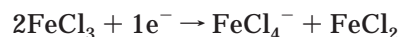
It is instructive to compare the absorption and luminescence spectra of PDOBTF with those reported for poly(fluorene)s and poly(fluoren-9-one-2,7-diyl) homopolymers. Poly(fluorene)s are blue emitters with a relatively low Stokes shift. The replacement of dialkyl groups with carbonyl ones at the 9-position results in a significant increase of the Stokes shift as observed in random copolymers of fluorene and fluoren-9-one²⁷ as well as in oxidatively degraded poly(fluorene)s.^{28–30} In both cases the keto groups act as "guest" emitters which efficiently trap singlet excitons created on the conjugated backbone by different types of excitation energy transfer mechanisms.^{29,30} Similar effects give rise to a large Stokes shift in poly(fluoren-9-one-2,7-diyl) homopolymer³¹ whose absorption band due to the backbone $\pi-\pi^*$ transition is located at 375 nm whereas the maximum of the photoluminescence band is at 580 nm. Thus, a very large Stokes shift in PDOBTF of ca. 245 nm, resulting in red emission, is not unexpected.

Finally, the influence of the head-to-head coupled 3-alkylthiophene rings on the optical properties of the copolymer studied should be briefly discussed. Evidently, the alkyl substituents create additional steric hindrance which results in an increase of the torsion angle along the polymer backbone. As a consequence, the absorption corresponding to the $\pi-\pi^*$ of the polymer backbone is hypsochromically shifted to 385 nm. Similar behavior is observed not only for head-to-head, tail-to-tail coupled poly(alkylthiophene) homopolymers³² but also for poly[(5,5'-(3,3'-dialkyl-2,2'-bithiophene))-*alt*-(2,7-(9,9-dialkylfluorene))]s which in their bithiophene segments are identical with our copolymer.⁵

Chemical Doping and Mossbauer Spectroscopy. UV-vis-NIR spectroelectrochemical data unequivocally show that the synthesized copolymer can be oxidatively doped; however, they do not indicate whether both subunits of the repeat unit, i.e., bithiophene and fluoren-9-one, undergo the oxidation. To address this problem, we have studied chemical doping of PDOBTF with FeCl_3 , combining elemental analysis, Mössbauer spec-

troscopy, and dc conductivity measurements.

With the goal to obtain the saturation or close to saturation doping level large excess of the doping agent was used. The most obvious phenomenological consequence of the doping process is the increase of the polymer conductivity over several orders of magnitude. This is also observed for the copolymer described here, whose RT dc conductivity reaches the value of 0.05 S cm^{-1} (measured on pressed powder). The mechanism of the doping of conjugated polymers with FeCl_3 has been described more than 20 years ago.³³ It involves a redox reaction accompanied by an acid-base one:



where P^+ denotes the segment of the polymer being oxidized to carbocation as a result of the doping. FeCl_4^- anions created according to the above reaction scheme diffuse to the polymer matrix in order to compensate the positive charge imposed on the polymer chain in the course of the doping process. Elemental analysis of doped PDOBTF is consistent with the above picture since the analytically determined Fe:Cl ratio is, within the experimental error, equal to 1:4. The doping level corresponds to 1.2 dopant anion (FeCl_4^-) per polymer repeat unit or equivalently to 6 dopants per 5 repeat units: Calcd for $\text{C}_{37}\text{H}_{42}\text{OS}_2(\text{FeCl}_4^-)_{1.2}$: %C, 55.23; %H, 5.22; %S, 7.96; %Cl, 21.20; %Fe, 8.36. Found: %C, 54.60; %H, 5.56; %S, 6.88; %Cl, 20.89; %Fe, 7.77.

Intuitively, one may expect that the charge introduced in the doping process should be localized on the bithiophene units which are easier to oxidize than the fluoren-9-one ones. This would however imply an unusually high charge concentration in the bithiophene segments, ca. 1 charge per 1.6 thiophene ring, which is approximately twice higher than typically observed in polythiophene homopolymers (1 charge per 3 thiophene rings). Thus, it can be postulated that in PDOBTF doped to saturation both subunits undergo the doping process or at least some fraction of the fluoren-9-one segments are doped. This postulate is consistent with Raman spectroscopic studies of the polymer doped to saturation. In this case the doping-induced shift toward lower wavenumbers is observed not only for the band at 1460 cm^{-1} ascribed to the $\text{C}_\alpha-\text{C}_\beta$ stretching deformations in the thiophene ring but also for the band at 1603 cm^{-1} originating from C-C stretching deformations in the aromatic ring of the fluoren-9-one subunit.

The doping of both subunits should also be manifested in ^{57}Fe Mössbauer spectra of the doped polymer.³⁴ It is known that both the isomer shift (IS) and the quadrupole splitting (QS) values in FeCl_4^- -doped conjugated polymers are dependent on the chemical constitution of the polycation neutralizing the charge of the dopant.³⁵ In particular, the IS values in doped heterocyclic and aromatic conjugated polymers are different. To the contrary, both IS and QS values are little dependent on the presence of alkyl substituents. These facts facilitate the assignment of the Mössbauer lines. Figure 5 shows the Mössbauer spectrum of doped PDOBTF. It can be deconvoluted into three doublets whose Mössbauer parameters are collected in Table 4. Two principal doublets of equal intensity are characteristic of high-spin Fe^{III} complexes and can be ascribed to FeCl_4^- at two different doping sites or, in other words, neutralized by carbocations of different nature. We ascribe the

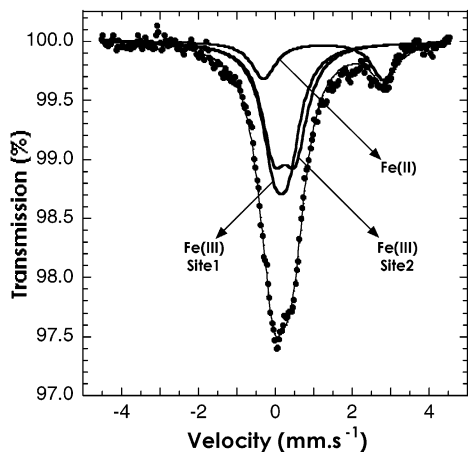


Figure 5. Mössbauer spectrum registered at 4.2 K of a PDOBTF thin film doped with FeCl_4^- .

Table 4. Mössbauer Parameters of PDOBTF Doped with FeCl_4^- ^a

	IS (mm s ⁻¹)	QS (mm s ⁻¹)	W (mm s ⁻¹)
Fe(III) site I	0.27 (2)	0.36 (2)	0.78 (2)
Fe(III) site II	0.37 (2)	0.57 (2)	0.78 (2)
Fe(II)	1.35 (2)	3.12 (2)	0.64 (2)

^a IS (isomer shift) relative to $\alpha\text{-Fe}$. QS (quadrupole shift) = $1/2e^2qQ$, W = line width. Errors are given in parentheses, in units corresponding to the last digit of quoted values.

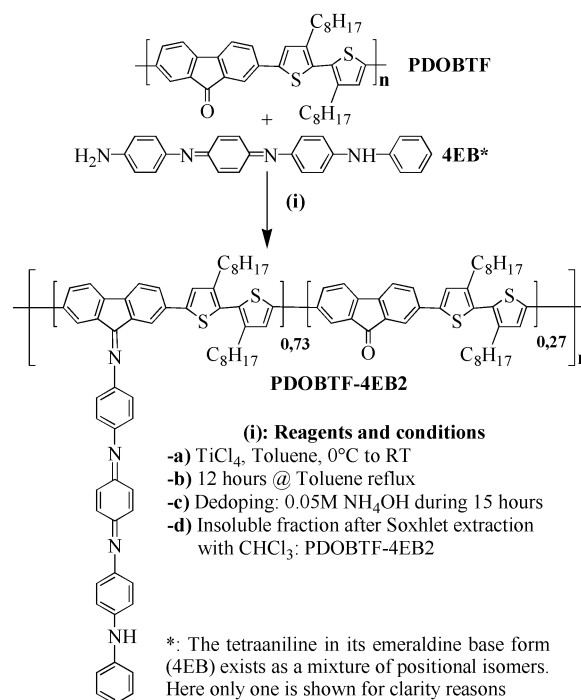
doublet with lower isomer shift (IS) and quadrupole shift (QS) values as originating from bithiophene doping sites since their Mössbauer parameters are close (but not identical) to those measured for poly(3-alkylthiophene) homopolymers.³⁵ The second $\text{Fe}^{(III)}$ doublet can in turn be attributed to FeCl_4^- associated with fluoren-9-one doping sites.³⁶ Much larger line widths measured for both doublets as compared to the case of conjugated homopolymers doped with the same dopant reflects the heterogeneous nature of the individual copolymer chain as well as a rather complex supramolecular structure of the doped polymer. Local changes in the polymer chain conformation as well as the coexistence of supramolecular aggregations of different degree of structural order result, for both doping sites, in a small distribution of the IS value around its mean value and by consequence contribute to the line broadening.

The third doublet of high isomer shift (IS = 1.35 mm s⁻¹) and a high quadruple splitting (QS = 3.12 mm s⁻¹) values, which accounts for ca. 15% of the intensity of the spectrum, is characteristic of $\text{Fe}^{(II)}$ and originates from incomplete removal of the side-reaction product (FeCl_2). Such incomplete removal of FeCl_2 is caused by minute amounts of water present in the doping solution which promote its precipitation within the polymer matrix.

At the end it should be stated that, in principle, other interpretations of the origin of the two observed principal $\text{Fe}^{(III)}$ doublets are possible. The explanation presented above seems to be the most plausible since it is supported by complementary spectroscopic data and is in accordance with Mössbauer spectroscopic data obtained previously for the corresponding homopolymers.

Postpolymerization Functionalization: Aniline Tetramer Grafting to PDOBTF Main Chain. One of the most interesting features of PDOBTF is the

Scheme 2. Postfunctionalization of PDOBTF with 4EB



possibility of precise tuning of its spectroscopic properties by grafting of appropriate chromophores via the carbonyl group present in the fluoren-9-one segment. In our first attempt to functionalize PDOBTF, we have selected aniline tetramer in the oxidation state of emeraldine (4EB) as the grafted chromophore. The presence of oligoaniline side groups not only influences the UV-vis-NIR spectrum of the polymer but also diversifies its electrochemical activity since in this case both the conjugated main chain and oligoaniline side chains are electroactive. Moreover, additional tuning of spectroscopic properties is possible by selective doping of the oligoaniline side chains via protonation.¹²

Oligoanilines can be conveniently attached to the chain of PDOBTF using TiCl_4 -catalyzed coupling reaction between the amine end group of the aniline tetramer and the carbonyl group of PDOBTF (see Scheme 2). A very similar procedure³⁷ has previously been applied to the synthesis of fluorenimines from fluoren-9-one and amines giving products in yields approaching 80%. In the case of the reaction between aniline tetramer and PDOBTF high grafting levels are obtained only after extended reaction times. The level of grafting can be conveniently determined by elemental analysis and in particular from the N/S ratio. An extended reaction time, ca. 12 h, applied in this research leads to a N/S molar ratio of 1.46, which corresponds to 73% grafting level, taking into account that each repeat unit of the polymer contains two sulfur atoms whereas each grafted oligoaniline group contains four nitrogen atoms. It should be noted here that "low grafting" level post-functionalized PDOBTF (PDOBTF-4EB1) remains solution processable in classical solvents of the polythiophene family of conjugated polymers (for example, THF, CHCl_3 , etc.) while the highest grafting level fraction (PDOBTF-4EB2: grafting level of ca. 73%) is soluble in solvents dissolving aniline oligomers such as *N*-methyl-2-pyrrolidinone (NMP).

In Figure 6a,b the IR spectrum of PDOBTF is compared with that registered for PDOBTF-4EB2.

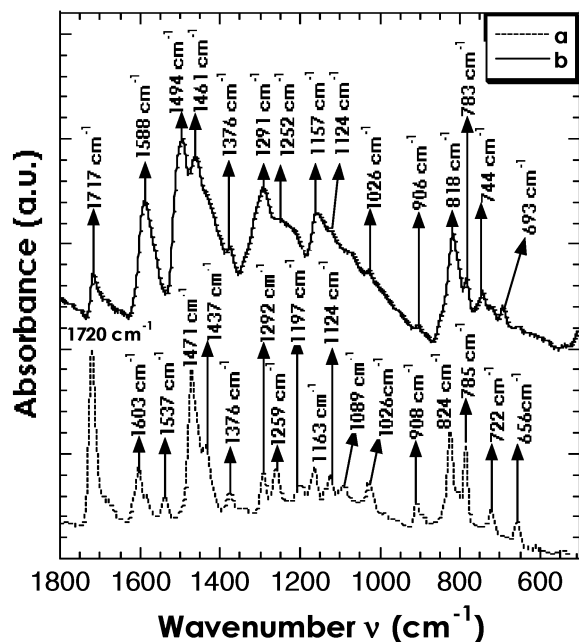


Figure 6. FTIR spectra (spectral range 500–1800 cm^{-1}) of PDOBTF (a) and postfunctionalized PDOBTF-4EB2 (grafting level 73%) (b).

Apart from the appearance of a broad band in the vicinity of 3340 cm^{-1} which is characteristic of N–H stretching deformations (not shown here), one can notice a significant decrease in the intensity of the band at 1717 cm^{-1} ascribed to >C=O stretchings in the carbonyl group, consistent with a rather high level of oligoaniline grafting which results in the transformation of the carbonyl linkages into the imine ones. Four most intensive bands characteristic of aniline tetramer at 1588 cm^{-1} , a doublet at 1494 and 1503 cm^{-1} , and a peak at 1291 cm^{-1} dominate in the spectrum of PDOBTF-4EB2 (compare parts a and b of Figure 6). The bands corresponding to the PDOBTF constituents, although less intensive, are also clearly visible. These are bands at 2916 and 2847 cm^{-1} (not shown here) originating from the C–H stretching deformations in the dialkylbithiophene units. Other bands characteristic of the alkyl groups are present at 1471 and 1376 cm^{-1} . The peaks associated with the deformations of the conjugated main chain can also be found in the spectrum, although in some cases they are obscured by the presence of the bands originating from the aniline tetramer deformations. This is for example the case of the band at 824 cm^{-1} attributed to out-of-plane deformations in the substituted thiophene ring which nearly coincides with a band characteristic of aniline tetramer at 818 cm^{-1} .

Grafting of aniline tetramer gives also rise to a significant modification of the UV–vis spectrum of the polymer (see Figure 7). In the spectrum of the polymer with an intermediate grafting level (PDOBTF-4EB1) we notice a new broad band peaked at 565 nm, which is characteristic of aniline tetramer in the oxidation state of emeraldine. This band is attributed to an excitonic transition between the HOMO level of the quinone ring and the LUMO level of the benzene ring. Consistent with a partial grafting reaction, this peak is superimposed on the peak at 476 nm, present in PDOBTF and ascribed to the $n-\pi^*$ transition of the carbonyl group. In the polymer with aniline tetramer side groups another electronic transition is also expected, namely

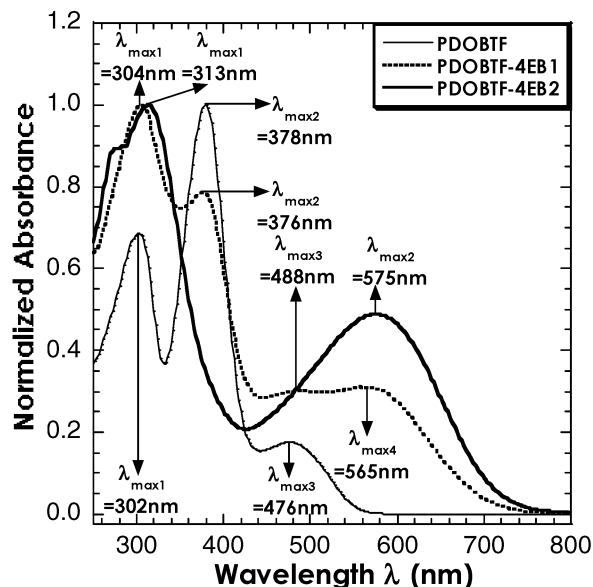


Figure 7. UV–vis solution (THF) spectra of PDOBTF, PDOBTF-4EB1 (“low grafting” level), and PDOBTF-4EB2 (grafting level 73%).

$\pi-\pi^*$ transition in the benzene ring. The band corresponding to this transition merges with the band characteristic of PDOBTF at 302 nm to give one broad peak with the maximum at 304 nm. This absorption peak strongly overlaps with the peak at 378 nm ascribed to the $\pi-\pi^*$ transition in the conjugated main chain. In the sample with the highest grafting level (73%) (PDOBTF-4EB2), the peaks originating from electronic transitions in the tetramer substituent dominate. The band due to the $\pi-\pi^*$ transition in the benzene ring of the tetramer merges in this case with the band originating from the $\pi-\pi^*$ transition in the main chain into one broad peak located at 313 nm.

In addition to the expected increase of the intensity of the bands originating from the tetramer with the increasing grafting level, one should note their bathochromic shift by ca. 10 nm as compared to the analogous bands registered, in the same experimental conditions, for the “free” tetramer, i.e., the tetramer not attached to the polymer chain. This shift unequivocally indicates the conjugation between the π -systems of the side groups and the main chain. Finally, the above-described experiments clearly demonstrate that the grafting reaction gives the opportunity of tuning the spectrum of the polymer both in the UV and in the visible regions.

Conclusions

To summarize, we describe in detail three methods of the preparation of a new regioregular conjugated copolymer, namely poly[(5,5'-(3,3'-di-*n*-octyl-2,2'-bithiophene))-*alt*-(2,7-fluoren-9-one)] (PDOBTF), which combines electronic properties of poly(flouren-9-one-2,7-diyl) homopolymer with solution processability of poly(alkylthiophene)s and in addition can be easily functionalized via carbonyl groups present in its main chain. SEC results show that, independent of the polymerization method (chemical or electrochemical oxidation of **(2)** or polycondensation of **(3)**), the resulting crude product is a mixture of high molecular weight fractions and short chain oligomers. It can however be fractionated into sharper fractions by sequential extraction. Upon doping the polymer becomes a conductor with the

conductivity $\sigma = 0.05 \text{ S cm}^{-1}$. We also demonstrate that postfunctionalization of PDOBTF consisting of aniline tetramer grafting to the main chain is a convenient method for tuning its spectroscopic properties.

Acknowledgment. The authors acknowledge ADEME and CEA for a partial funding (Convention de recherche No. 0105148) through the CSPVP "Cellules Solaires Photovoltaïques Plastiques" research program. We also thank C. Lebrun for her assistance in MS-ESI characterizations and helpful discussions.

References and Notes

- (1) Bao, Z. *Adv. Mater.* **2000**, *12*, 227–230.
- (2) Kraft, A. C.; Grimsdale, A. C.; Holmes, A. B. *Angew. Chem., Int. Ed.* **1998**, *37*, 402–428.
- (3) Yu, G.; Hummelen, J. C.; Wudl, F.; Heeger, A. J. *Science* **1995**, *270*, 1789–1791.
- (4) Uckert, F.; Setayesh, S.; Müllen, K. *Macromolecules* **1999**, *32*, 4519–4524.
- (5) Liu, B.; Yu, W. L.; Lai, Y. H.; Huang, W. *Macromolecules* **2000**, *33*, 8945–8952.
- (6) Pei, J.; Yu, W. L.; Huang, W.; Heeger, A. J. *J. Chem. Soc., Chem. Commun.* **2000**, 1631–1632.
- (7) Wong, K. T.; Chien, Y. Y.; Chen, R. T.; Wang, C. F.; Lin, F. T.; Chiang, H. H.; Hsieh, P. Y.; Wu, C. C.; Chou, C. H.; Su, Y. O.; Lee, G. H.; Peng, S. M. *J. Am. Chem. Soc.* **2002**, *124*, 11576–11577.
- (8) Brabec, C. J.; Sariciftci, N. S.; Hummelen, J. C. *Adv. Funct. Mater.* **2001**, *11*, 15–26.
- (9) Brabec, C. J.; Cravino, A.; Meissner, D.; Sariciftci, N. S.; Fromherz, T.; Rispens, M. T.; Sanchez, L.; Hummelen, J. C. *Adv. Funct. Mater.* **2001**, *11*, 374–380.
- (10) Padinger, F.; Rittberger, R. S.; Sariciftci, N. S. *Adv. Funct. Mater.* **2003**, *13*, 85–88.
- (11) Feng, J.; Zhang, W.; MacDiarmid, A. G.; Epstein, A. J. *Proc. Soc. Plast. Eng., Annu. Technol. Conf. (ANTEC 97)* **1997**, *2*, 1373–1377.
- (12) Dufour, B.; Rannou, P.; Travers, J. P.; Pron, A.; Zagorska, M.; Korc, G.; Kulszewicz-Bajer, I.; Quillard, S.; Lefrant, S. *Macromolecules* **2002**, *35*, 6112–6120.
- (13) Jayakannan, M.; Van Dongen, J. L.; Janssen, R. A. *Macromolecules* **2001**, *34*, 5386–5393.
- (14) Asawapirom, U.; Günter, R.; Forster, M.; Farrell, T.; Scherf, U. *Synthesis* **2002**, *9*, 1136–1142.
- (15) Guillerez, S.; Bidan, G. *Synth. Met.* **1998**, *93*, 123–126.
- (16) Bäuerle, P.; Pfau, F.; Schupp, H.; Wurthner, F.; Gaudl, K. U.; Balparda Caro, M.; Fischer, P. *J. Chem. Soc., Perkin Trans. 2* **1993**, 489–494.
- (17) Andersson, M. R.; Selse, D.; Berggren, M.; Jarvinen, H.; Hjertberg, T.; Inganäs, O.; Wennerström, O.; Osterholm, J. E. *Macromolecules* **1994**, *27*, 6503–6506.
- (18) Yamamoto, T. *Bull. Chem. Soc. Jpn.* **1999**, *72*, 621–638.
- (19) Shiraishi, K.; Yamamoto, T. *Synth. Met.* **2002**, *130*, 139–147.
- (20) Zhang, Z. B.; Fujiki, M.; Tang, H. Z.; Motonaga, M.; Torimitsu, K. *Macromolecules* **2002**, *35*, 1988–1990.
- (21) Yong-Joo Kim, R.; Sato, R.; Maruyama, T.; Osakada, K.; Yamamoto, T. *J. Chem. Soc., Dalton Trans.* **1994**, 943–948.
- (22) Liu, J.; Loewe, R. S.; McCullough, R. D. *Macromolecules* **1999**, *32*, 5777–5785.
- (23) Trznadel, M.; Pron, A.; Zagorska, M.; Chrzaszcz, R.; Pieli-chowski, J. *Macromolecules* **1998**, *31*, 5051–5058.
- (24) Hourquebie, P.; Olmedo, L. *Synth. Met.* **1991**, *65*, 19–26.
- (25) Ishikawa, H.; Amano, K.; Kobayashi, K.; Satoh, A.; Hasegawa, E. *Synth. Met.* **1994**, *64*, 49–52.
- (26) See, for example: Inganäs, O. In *Handbook of Organic Conductive Molecules and Polymers*; Nalwa, H., Ed.; Wiley & Sons: New York, 1997; Vol. 3, p 785.
- (27) Panozzo, S.; Vial, J. C.; Kervella, Y.; Stéphan, O. *J. Appl. Phys.* **2002**, *92*, 3495–3502.
- (28) Bliznyuk, V. N.; Carter, S. A.; Scott, J. C.; Klärner, G.; Miller, R. D.; Miller, D. C. *Macromolecules* **1999**, *32*, 361–369.
- (29) List, E. J. W.; Guentner, R.; Scandiucci de Freitas, P.; Scherf, U. *Adv. Mater.* **2002**, *14*, 374–378.
- (30) Zojer, E.; Pogantsch, A.; Hennebicq, E.; Beljonne, D.; Brédas, J. L.; Scandiucci de Freitas, P.; Scherf, U.; List, E. J. W. *J. Chem. Phys.* **2002**, *117*, 6794–6802.
- (31) Uckert, F.; Tak, Y. H.; Müllen, K.; Bäessler, H. *Adv. Mater.* **2000**, *12*, 905–908.
- (32) Lapkowski, M.; Zagorska, M.; Kulszewicz-Bajer, I.; Pron, A. *J. Electroanal. Chem.* **1992**, *341*, 151–163.
- (33) Pron, A.; Zagorska, M.; Kucharski, Z.; Lukasiak, M.; Suwalski, J.; *Mater. Res. Bull.* **1982**, *17*, 1505–1510.
- (34) Greenwood, N. N.; Gibbs, T. C. In *Mössbauer Spectroscopy*; Chapman and Hall: London, 1971.
- (35) Kulszewicz-Bajer, I.; Pron, A.; Suwalski, J.; Kucharski, Z.; Lefrant, S. *Synth. Met.* **1989**, *28*, C225–C229.
- (36) Pron, A.; Fatseas, G.; Krichene, S.; Lefrant, S.; Maurice, F.; Froyer, G. *Phys. Rev. B* **1985**, *32*, 1839–1842.
- (37) Dai, W.; Srinivasan, R.; Katzenellenbogen, J. A. *J. Org. Chem.* **1989**, *54*, 2204–2208.

MA030171Z